Zero sequence blocking transformers for multi-pulse rectifier in aerospace applications

Yao, Wenli; Blaabjerg, Frede; Zhang, Xiaobin; Yang, Yongheng; Gao, Zhaohui

Published in:
Proceedings of the 2014 IEEE Energy Conversion Congress and Exposition (ECCE)

DOI (link to publication from Publisher):
10.1109/ECCE.2014.6953508

Publication date:
2014

Document Version
Early version, also known as pre-print

Zero Sequence Blocking Transformers for Multi-Pulse Rectifier in Aerospace Applications

Wenli Yao†, Frede Blaabjerg‡, Xiaobin Zhang†, Yongheng Yang‡, Zhaohui Gao†

†School of Automation
Northwestern Polytechnical University
127 Youyi West Road, Xi'an, Shaanxi, 710072, P.R. China
mjkfhill@live.com, dgl907@126.com, holly@nwpu.edu.cn

‡Department of Energy Technology
Aalborg University
Pontoppidanstraede 101, Aalborg, DK-9220 Denmark
fbl@et.aau.dk, yoy@et.aau.dk

***Abstract* – Auto-Transformer Rectifier Units (ATRU) have been widely adopted in aircrafts due to its simplicity and reliability. In this paper, Zero Sequence Blocking Transformers (ZSBT) are employed in the DC link to realize parallel rectifier bridges for ATRU, being the proposed 24-pulse rectifier. A star-connected autotransformer is used in this topology to divide the primary side voltage into four three-phase voltage groups, among which there is a phase shift of 15°. The autotransformer then feeds the load through rectifier bridges, which are in parallel with ZSBTs. Compared to the traditional method that is using six interphase transformers to parallel the rectifier bridges, the proposed 24-pulse rectifier only requires four ZSBTs. This will contribute to a reduction of weight and cost of the entire system. The operation principle of the ZSBT is analyzed, and the kVA rating design of each component in the proposed unit is also explored. The kVA rating of ZSBT is only 0.034 times of the rated power. Moreover, this topology can eliminate low-order harmonics in the AC supply current. An 18 kW prototype is built up for tests. Both simulations and experiments have verified the main features of the proposed 24-pulse rectifier in terms of higher efficiency, higher power factor and lower total harmonic distortions.**

***Index Term*-- Autotransformer rectifier units, Zero sequence blocking transformers, Multi-pulse rectifier, 24-pulse rectifier, Aerospace application.**

I. INTRODUCTION

With the development of More Electric Aircrafts (MEA), aircraft electrical distribution system capacity increases dramatically to replace hydraulic, pneumatic and mechanical systems onboard. MEA has the advantages of increased reliability, maintainability, supportability, as well as reduced weight and volume [1], [2]. The Boeing 787 Dreamliner (B787), for example, is a typical representation of mostly electrical flight systems with a high penetration of power electronics, multi-level voltage and hybrid DC and AC systems. To eliminate the mechanical constant speed shaft for constant frequency generator, the variable frequency generators technology is adopted in the B787 and Airbus 380 (A380) [3], [4]. Thus, the electrical system of MEA is a mixed-voltage system, which consists of four types of voltage: 230 VAC, 115 VAC, 28 VDC and 270 VDC. The role of power electronics is to convert the variable-frequency power into different voltages from the generator. Thus, AC-DC converters are widely used in MEA. There are mainly two types of AC-DC conversion systems on board – Pulse Width Modulation (PWM) converter and Auto-Transformer Rectifier Unit (ATRU). The later one has been widely adopted in military and commercial aircrafts, due to its simplicity, reliability, maintainability and reduced kVA ratings [5]. In the B787, ATRUs are used to feed the adjusted speed loads, e.g., hydraulic pump motor and engine start. Since the ATRU consists of rectifier bridges and autotransformer without isolation, the rectifiers should be designed with a higher number of pulses in order to maintain low Total Harmonic Distortions (THD) of the AC current and almost ripple-free DC voltage [5], [6].

In view of the above concerns, this paper firstly proposes a cost-effective autotransformer based multi-pulse rectifier (24-pulse) for ATRU applications. The secondary of the autotransformer is divided into four three-phase groups, and each consists of three balanced voltages with a 15° phase shift among them. The output of the autotransformer feeds four three-phase six-pulse rectifier bridges. The Zero Sequence Blocking Transformers (ZSBT) [7] is designed to ensure independent operation of the diode bridge rectifiers in rectifier parallel system as well as to promote equal current sharing. A multi-tap InterPhase Reactor (IPR) is another way to connect two rectifiers in parallel. If the tap number is n, then the pulse number of AC-DC converter is $12n$. However, its design procedure and winding structure is much complicated [8]. Two windings InterPhase Transformer (2-IPTs) have usually been chosen for two-parallel rectifiers, and the interest in multi-windings InterPhase Transformer (N-IPTs) is growing with the demand of multi-paralleled connections. 2-IPTs and N-IPTs topologies have been proposed, modeled and analyzed in [9] and [11]. Both IPT topologies require a symmetrical geometric structure of the core. N-IPTs are usually constructed by connecting 2-IPTs, which are only applicable to 12-pulse converters. Thus, an active IPT for paralleled rectifiers in multi-pulse converters was introduced in [12]. However, its control is more complicated compared to the traditional IPTs, and thus the overall reliability is reduced.

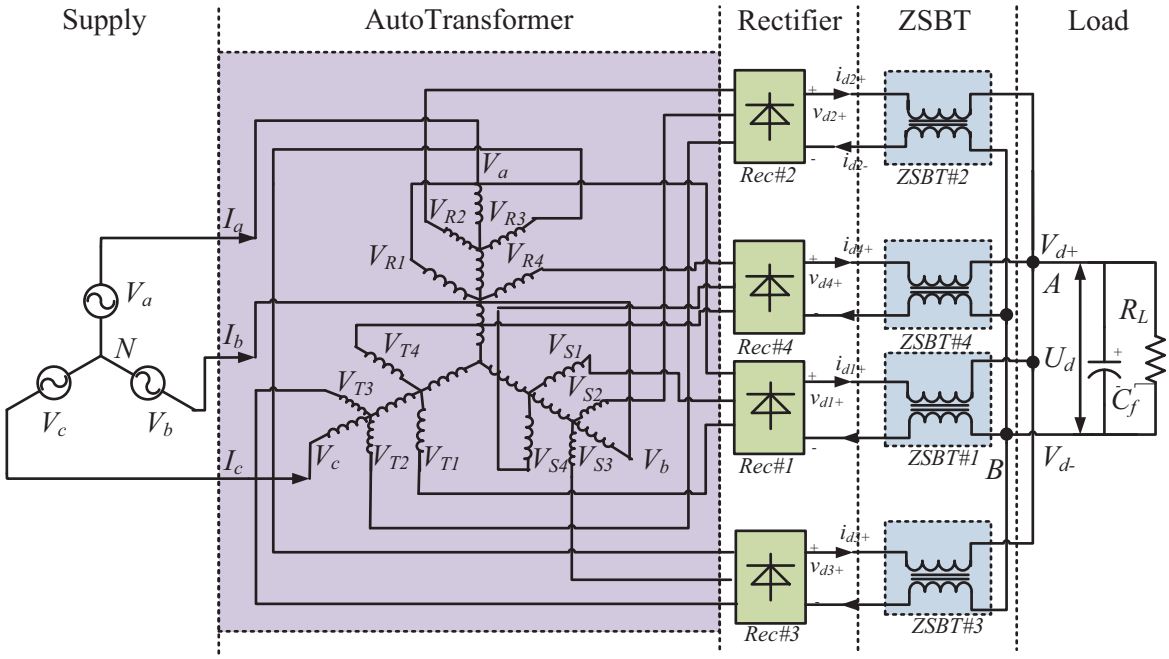

Fig. 1. Proposed hardware schematics of the 24-pulse Auto-Transformer Rectifier Unit (ATRU).

In order to solve the above issues, a ZSBT is developed for the proposed 24-pulse ATRU in this paper. The number of ZSBTs is reduced to four compared to the one (i.e. six 2-IPTs) employed in [13]. Besides, there is no need to consider flux symmetrical issue for implementations when compared to the 2-IPT and N-IPT. The operation principle of the proposed converter is illustrated in § II. The operation principle and kVA rating design of the ZSBT is analyzed in § III. Simulations and experimental results are provided in § IV to validate the effectiveness of the proposed topology in terms of harmonics suppressions, reduced number of ZSBTs, system volume, and cost.

II. System Description

Fig. 1 shows the proposed 24-pulse ATRU, which consists of an autotransformer and four rectifier Bridges with ZSBTs. In this configuration, the secondary of the autotransformer is divided into four three-phase groups. Each group consists of three balanced voltages with 15° phase shift among them [14], and it is connected to a three-phase six-pulse rectifier bridge. The DC outputs of all rectifier bridges are connected in parallel through ZSBTs to feed the load in order to achieve the required pulse multiplication effects and harmonic cancellation benefits. It can be seen that the proposed topology can produce a 24-pulse voltage. It should be mentioned that the use of ZSBTs is to ensure an independent six-pulse (i.e., 120° -conduction) operation of each rectifier bridge, and also to achieve equal current sharing among different phases.

A. Design of Autotransformer

The connection of star-autotransformer is shown in Fig. 1. Each group of secondary voltages in this configuration can produce a phase shift of 15° among other groups [14]. Rectifier bridges *Rec#1* to *Rec#4* are connected to the autotransformer [13], [14]. The winding connection and vector diagram of the autotransformer are briefly depicted in Fig. 2, where K_1, K_2, K_3 and K_4 are the fractions of the phase voltages, representing the turns-ratio of the winding in respect to the primary voltage. Assuming that the line voltages V_a, V_b and V_c are ideal, they can be expressed as,

$$\begin{cases} V_a = V_m \sin \omega t \\ V_b = V_m \sin\left(\omega t - 2\pi/3\right) \\ V_c = V_m \sin\left(\omega t + 2\pi/3\right) \end{cases} \quad (1)$$

where V_m and ω are peak value and frequency of input phase voltage. As it is shown in Fig. 1 and Fig. 2, the three-phase voltage $[V_{R1}, V_{S1}, V_{T1}]$, $[V_{R2}, V_{S2}, V_{T2}]$…$[V_{R4}, V_{S4}, V_{T4}]$ are the outputs of the autotransformer. The voltages of V_{R1}, V_{R2}, V_{R3}, V_{R4} have a phase shift of 15° among each other and can be given as,

$$V_{Ri} = V_m \sin[\omega t + \frac{(2i-5)\pi}{24}] \quad (2)$$

in which $i=1,2,3,4$ represent the autotransformer output group number as shown in Fig. 1. Based on (1) and (2), K_1, K_2, K_3 and K_4 can be calculated, and the results are shown in Table I, where the other parameters of the autotransformer are also presented. Then, all the output voltages of the auto-transformer can be obtained.

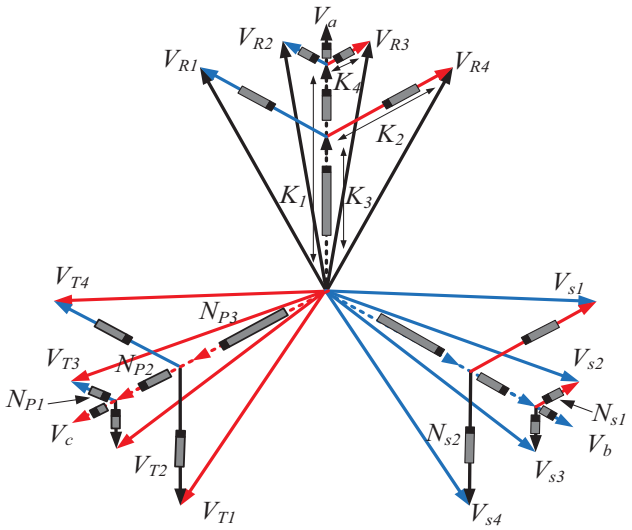

Fig. 2. Winding connection and phasor diagram of the autotransformer.

For instance, the voltage $\vec{V}_{R3}$ can be obtained by tapping phase A ($K_1\vec{V}_a$) and phase C ($K_4\vec{V}_c$), i.e. $\vec{V}_{R3} = K_1\vec{V}_a + K_4\vec{V}_c$. As it is shown in Table I, the kVA rating of the autotransformer (4.7 kVA) only accounts for 27 % of the load power (18 kW). Since the magnetic core processes only about 4.7 kVA, the proposed topology results in reduced weight and volume. Otherwise, by using K_1~K_4, the parameter of winding can be determined, the turns and current of primary (N_{p1}, N_{p2} and N_{p3}) and secondary windings (N_{s1} and N_{s2}) are shown in Table III.

TABLE I
PARAMETERS OF AUTOTRANSFORMER

Parameter	Value
Input Voltage	3-φ,115 V/400 Hz
Output Voltage	4-group 3-φ, 115 V/400 Hz
Load Power	18 kW
Power of Core	4.7 kVA
Weight of core	17.6 kg
Core Size	EE 40*40*100 mm
Autotransformer size	118*260*240 mm
Material	0.2 mm Silicon Strip
B_m	1.2 T
K_1, K_2, K_3 , K_4	0.9619, 0.1507, 0.7029, 0.4419,

B. Analysis of Input Current

According to the autotransformer output voltages given in (1) and (2), on the assumption that a highly inductive load is connected at the rectifier outputs, the rectifier input currents can be represented as [15],

$$\begin{cases} I_{Ri} = \sum_{n=1,3,5,\ldots}^{\infty} [\frac{4I_{di}}{n\pi}\cos(\frac{n\pi}{6})]\sin n(\omega t + \frac{(2i-5)\pi}{24}) \\ I_{Si} = \sum_{n=1,3,5,\ldots}^{\infty} [\frac{4I_{di}}{n\pi}\cos(\frac{n\pi}{6})]\sin n(\omega t + \frac{(2i-21)\pi}{24}) \\ I_{Ti} = \sum_{n=1,3,5,\ldots}^{\infty} [\frac{4I_{di}}{n\pi}\cos(\frac{n\pi}{6})]\sin n(\omega t + \frac{(2i+11)\pi}{24}) \end{cases} \quad (3)$$

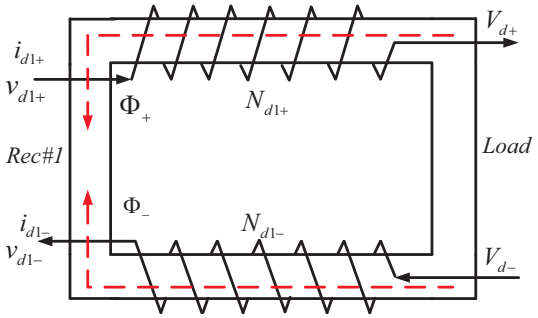

Fig. 3. Winding configuration of the zero sequence blocking transformers.

where I_{di} is the output current of rectifier bridge, i=1, 2, 3, 4. Referring to Fig. 1 and Fig. 2 and by neglecting the magnetizing current, the input current I_a for phase "a" of the autotransformer is given by,

$$I_a = K_1(I_{R1} + I_{R3}) + K_3(I_{R2} + I_{R4}) - K_2(I_{T1} + I_{S3}) - K_4(I_{T2} + I_{S4}) \quad (4)$$

Substituting (2) and (3) into (4), the input current I_a can then be expressed as,

$$I_a = 2\sum_{n=1,3,5,\ldots}^{\infty} A_n \cdot \sin(n\omega t) \quad (5)$$

and,

$$A_n = \left(\frac{I_d}{n\pi}\cdot\cos\frac{n\pi}{6}\right)\left(K_1\cos\frac{1}{24}n\pi + K_3\cos\frac{1}{8}n\pi - K_2\cos\frac{17}{24}n\pi - K_4\cos\frac{19}{24}n\pi\right) \quad (6)$$

in which I_d is the output DC current. It can be calculated according to (6) that A_5, A_7, A_{11}, A_{13}, A_{17}, A_{19} are almost zero, and A_{23}, A_{25} are about 0.04 I_d. Therefore, the harmonics of the input current only consist of the 24k±1-order harmonics (k=1, 2, 3, …). The odd-order harmonics (i.e. 5th, 7th, 11th, 13th, 17th, 19th, and 21st) will be eliminated in the input currents.

C. Zero Sequence Blocking Transformers (ZSBT)

The proposed ZSBT consists of two windings as it is shown in Fig. 3. In contrast to the conventional IPTs, both windings of the proposed ZSBT are connected to the rectifier. This ensures that the rectifier can operate independently, the diodes in each rectifier bridge conduct for 120 degrees per cycle and the rectifier carries one-fourth of the load current, thus leading to a reduced ZSBT rating. The turns of these two windings are equal to opposite directions. According to the Ampere's law, DC flux in the core is also equal and opposite. It is possible to select a smaller core for the ZSBT and reduce the weight and volume of the system.

III. ANALYSIS OF ZERO SEQUENCE BLOCKING TRANSFORMERS

A. Analysis voltage and current of ZSBT

Referring to Fig. 3, the windings of the ZSBT are denoted as N_{d1+} and N_{d1-}. The winding current can be decomposed into AC and DC components. For the DC component, it will not induce any voltage drop. For the AC component current

(circulating current), it can be decomposed into i_{dl+} and i_{dl-} respectively. The current i_{dl+} is excited by the winding voltage V_{N1+}, which can be given by,

$$V_{N1+} = L_{N1+}\frac{di_{d1+}}{dt} - M_1\frac{di_{d1-}}{dt} \tag{7}$$

in which, M_1, L_{N1+} and L_{N1-} are the mutual and self-inductance between $N_{dl+}$and N_{dl-}. In addition, the other ZSBT winding voltage can be obtained. These four ZSBTs have the same structure and windings, and thus the mutual and self-inductance is also approximately equal. Those can be denoted as L and M. The voltage relationship between the converter and rectifier is expressed by,

$$V_{d+}(t) = v_{di+} - V_{Ni+} \qquad i = 1,...,4 \tag{8}$$

where V_{d+} and v_{di+} are the voltages with respect to the neutral point ***N***. From (7) and (8), the voltage of node ***A*** shown in Fig. 1 is calculated as,

$$V_{d+}(t) = \frac{1}{4}\left[\sum v_{di+} + L\sum\frac{di_{di+}}{dt} + M\sum\frac{di_{di-}}{dt}\right] i = 1,...,4 \tag{9}$$

since the circulating current excited by rectifier output instantaneous voltages only exists between rectifiers and not flow into the load, thus at the parallel node ***A*** and ***B*** in Fig. 1, according to Kirchhoff's current law, the currents can be given as,

$$\sum i_{di+} = \sum i_{di-} = 0 \tag{10}$$

Then, Eq. (9) can be simplified as,

$$V_{d+}(t) = \frac{1}{4}\sum v_{di+} \qquad i = 1,...,4 \tag{11}$$

where V_{d+} is the average voltage of v_{di+}. Since the positive output voltage of the full bridge rectifier is equal to a three-phase half-bridge rectifier, according to (1) and (2), the Fourier series expansion of v_{di+} can be given by [13],

$$v_{di+} = \frac{3\sqrt{3}}{2\pi}V_m[1 - \sum_{j=1}^{\infty}\frac{2\cos j\pi\cos(3j(\omega t + \frac{(2i-5)\pi}{24}))}{(3j)^2 - 1}] \tag{12}$$

in which, V_m is peak value of input phase voltage. From (11) and (12), the voltages of V_{d+} and V_{d-} can be obtained, and then the output voltage of converter can be expressed as,

$$U_d(t) = V_{d+} - V_{d-} = \frac{3\sqrt{3}}{\pi}V_m[1 + \sum_{j=1}^{\infty}\frac{\cos j24\omega t}{(24j)^2 - 1}] \tag{13}$$

Eq. (13) indicates that the lowest harmonic order is the 24th one and the ripple voltage is about 0.12% in respect to the DC value. The voltage of the ZSBT winding is determined by,

$$V_{Ni+}(t) = v_{di+} - V_{d+} \tag{14}$$

According to (11) and (12), V_{N1+} and V_{N1-} can be expressed as,

$$V_{N1+}(t) = \frac{3\sqrt{3}}{2\pi}V_m[0.117\cos(3\omega t - 32.23) - 0.014\cos 6\omega t + 0.028\cos(9\omega t + 12.76) + ...] \tag{15}$$

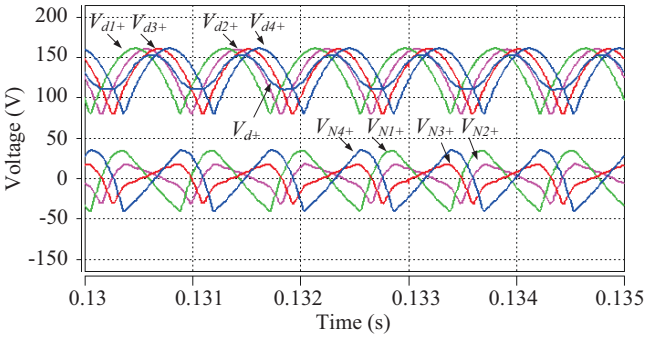

Fig. 4. Voltages across the zero sequence blocking transformers.

$$V_{N1-}(t) = -\frac{3\sqrt{3}}{2\pi}V_m[-0.117\cos(3\omega t - 32.23) + 0.014\cos 6\omega t + 0.028\cos(9\omega t - 12.76) + ...] \tag{16}$$

Since the four outputs of autotransformer have different phase shifting angle relative to power supply, the voltage of the ZSBT winding are quite different as shown in Fig. 4.

The voltages of *ZSBT#2* and *ZSBT#3* are much lower than *ZSBT#1* and *ZSBT#4*, and from (15), the RMS value across *ZSBT#2* and *ZSBT#3* can be given as,

$$V_{N2+} = V_{N3+} = 0.121V_m \tag{17}$$

Using the same calculation procedure, the RMS value across *ZSBT#1* and *ZSBT#4* are obtained as *0.186* V_m. These values are used to calculate the turns-ratio of ZSBT windings. Eqs. (15) and (16) indicate that the fundamental frequency of ZSBT winding is the tripled frequency of the converter input, while the phase and magnitude of the fundamental component is equal. Thus, the total AC flux in the core is nine times of the input frequency, and it is relatively small. This will contribute to a reduced size of ZSBTs. It should be noted that the ZSBT winding voltages given in (15) and (16) are based on the assumption that the input primary voltages are ideal.

Take the AC component as voltage sources, which are denoted as $\dot{V}_{L+}$ and $\dot{V}_{L-}$. The decoupled equivalent circuit of the ZSBT is shown in Fig. 5(a). $\dot{I}_1$ and $\dot{I}_2$ are the AC components of the ZSBT winding current. L_{N+} and L_{N-} are the self-inductance of ZSBT windings, and they are equal to L. According to the Superposition theorem short circuit voltage source $\dot{V}_{N-}$ and the equivalent circuit is shown in Fig 5(b), $\dot{I}_1'$ and $\dot{I}_2''$ is the left and right branch current respectively. According to the Kirchhoff's current law, the voltage $\dot{V}_{N+}$ can be expressed as,

$$\dot{V}_{N+} = \dot{I}' \times j\omega L(1 - k^2) \tag{18}$$

where $k = M/\sqrt{L_{N+}L_{N-}} = M/L$ is the coupling coefficient. The short circuit voltage source $\dot{V}_{N+}$ and the equivalent circuit are shown in Fig. 5(c), $\dot{I}_2'$ and $\dot{I}_1''$ are the left and right branch current respectively. According to the Kirchhoff's current law,

$$\dot{V}_{N-} = \dot{I}_2' \times j\omega L(1-k^2) \tag{19}$$

In accordance to Fig. 5(c), $\dot{I}_1''$ can be expressed as,

$$\dot{I}_1'' = \frac{-k\dot{V}_{N-}}{j\omega L(1-k^2)} \tag{20}$$

based on the Superposition theorem, $\dot{I}_1$ and $\dot{I}_2$ can be given as,

$$\dot{I}_1 = \frac{\dot{V}_{N+}}{j\omega L(1-k^2)} + \frac{k\dot{V}_{N-}}{j\omega L(1-k^2)} = \dot{I}_1' + k\dot{I}_2'' \tag{21}$$

$$\dot{I}_2 = \frac{\dot{V}_{L-}}{j\omega L(1-k^2)} + \frac{k\dot{V}_{L+}}{j\omega L(1-k^2)} = \dot{I}_2' + k\dot{I}_1'' \tag{22}$$

where k is the coupling coefficient.

B. Turns and kVA rating of ZSBT

From (18) ~ (22), it can be seen that the coupling coefficient k is highly relevant to the AC components of ZSBT current. A small coupling coefficient will contribute to lower AC components of ZSBT winding current, and thus continuous diode current during the conduction period. This may help to lower the copper loss of ZSBT and to improve the input current quality at the low power condition. According to the analysis above, both AC and DC flux of the ZSBT core are small, and the winding voltage is fixed. In order to calculate the turns of ZSBT, the following constraint condition which should be fulfilled is that the electromotive force of the winding must be larger than the winding voltage V_N,

$$V_N < E = 4.44 f N B_m A \tag{23}$$

in which f is the frequency of the ZSBT voltage, N is the turn, B_m is the maximum flux density, E is the electromotive force of winding and A is the core area. The constraint in (23) determines the minimum value of ZSBT winding turns. Table II shows the results of designed ZSBTs considering the condition of (23), and the corresponding turns of ZSBT windings are also listed in Table III.

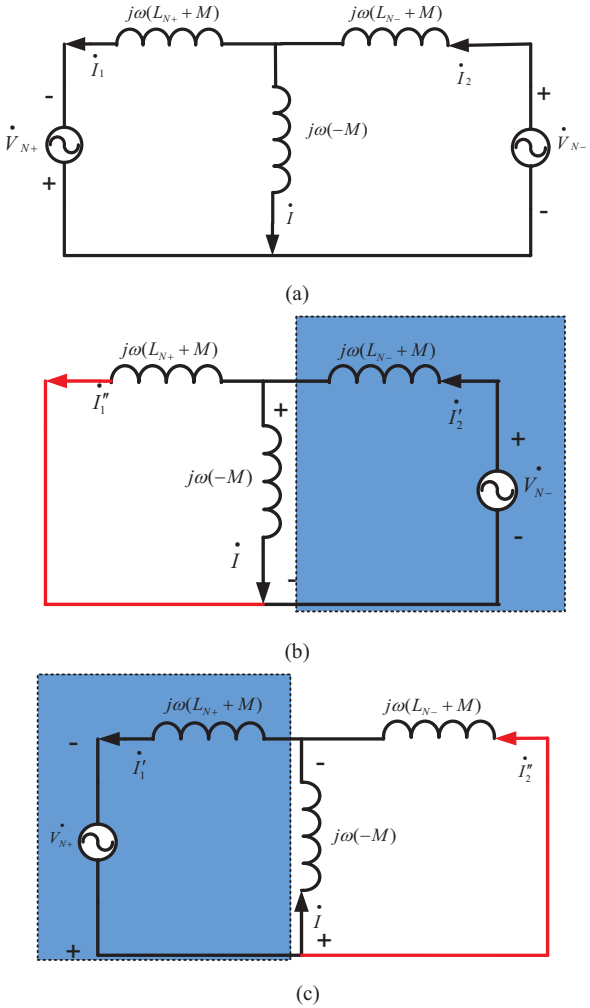

Fig. 5. Equivalent circuits of the zero sequence blocking transformers: (a) decoupled equivalent circuit, (b) equivalent circuit (N_+ short circuit), and (c) equivalent circuit (N_- short circuit).

TABLE II
PARAMETERS OF ZERO SEQUENCE BLOCKING TRANSFORMERS.

Parameter	Value
Power of Core	0.6 kVA
kVA rating	0.034 P_O
Material	Ferrite
B_m	0.5 T
Core Size	Toroidal Core ID:40;OD:55
Weight of core	0.6 kg
Radius of *ZSBT*	62 mm
N_+, N_-	54

To compute the kVA rating of the ZSBTs, the RMS voltage and RMS current are necessary. Since a quarter of the load current flows through each winding of the ZSBT, the kVA rating of the ZSBT can be obtained by,

$$kVA_{ZSBT} = \frac{1}{2}\sum_{i=1}^{4}\frac{1}{4} I_O \cdot V_{Ni+} = 0.034 P_o \tag{24}$$

it should be noted that the total kVA rating of ZSBTs is quite small and also the frequency is triple of the source frequency as shown in (12). Both will contribute to a smaller size of ZSBT core, and thus reduced total cost and improved performance.

TABLE III
PARAMETERS OF THE AUTOTRANSFORMER WINDING.

Winding	N_{p1}	N_{p2}	N_{p3}	N_{s1}	N_{s2}	N_d+	N_{d-}
Turns	5	13	43	9	27	54	54
Current (A)	55.4	27.5	2.3	13.6	13.6	16.7	16.7

IV. SIMULATION AND EXPERIMENTAL RESULTS

In order to verify the proposed configuration, simulations and experiments are carried out. The specifications of the system are: voltage = 115 V_{RMS}; input voltage frequency: 360 Hz~800 Hz; P_o =18 kW; input current THD ≤ 10%. The designed parameters are shown in Tables I, II, and III. The turns of autotransformer should be integer in order to avoid phase and magnitude error in the autotransformer output,

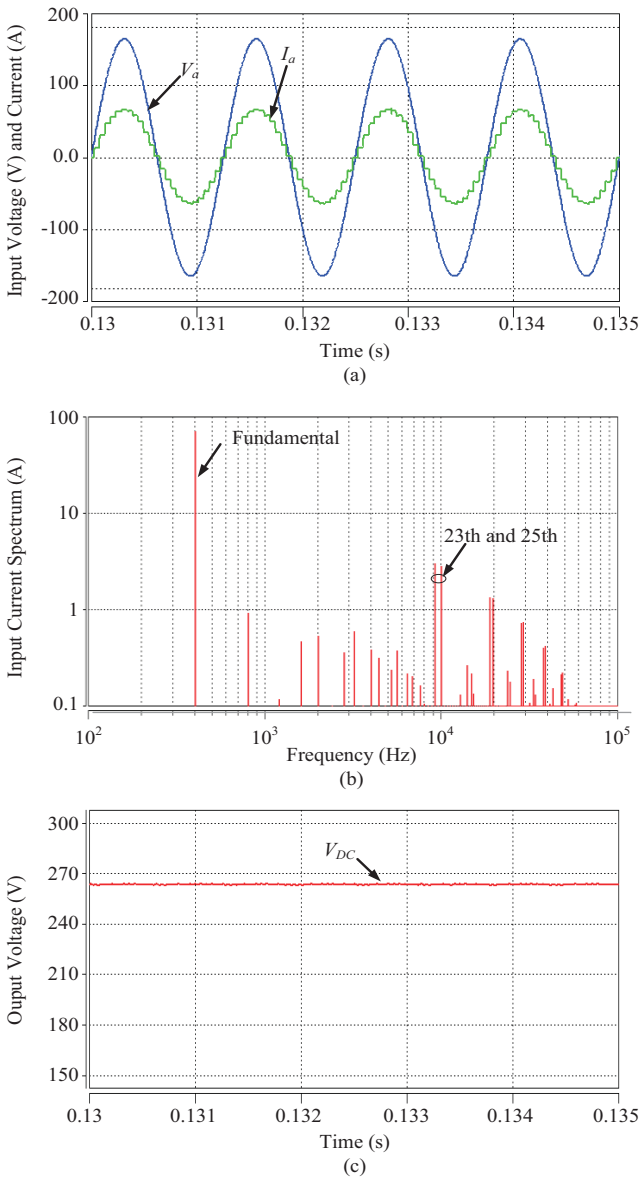

Fig. 6. Simulation results of the 24-pulse Auto-Transformer Rectifier Units at full load: (a) phase A input current and voltage, (b) phase A current spectrum, and (c) Auto-Transformer Rectifier Units output voltage.

since the phase and magnitude error may cause current unbalance between rectifiers, which requires larger winding wire for ZSBT and thus leading to increased size of the ZSBT core. The autotransformer and ZSBT are modeled using Magnet Component Tool in Saber software with the parameters shown in Table I and Table II. Fig. 6 shows the simulation results of the proposed 24-pulse ATRU at full load operation. The THD of the line current I_a is 7.42 %, where harmonics lower than 23rd are suppressed effectively. The output waveform is shown in Fig. 6 (c) indicates that the ripple voltage is about 0.14% in respect to the DC value.

With the parameters shown in Table I, an 18 kW ATRU has been implemented. Fig. 7 shows the system layout of the

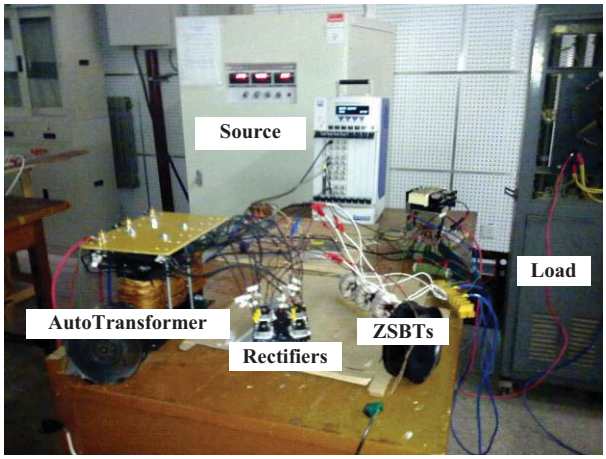

Fig. 7. Experimental setup of the 18-kW proposed 24-pulse autotransformer rectifier units (ATRU).

experimental setup. The test setup includes a 24-pulse phase-shifting autotransformer, which is fed by 60-kVA power source, and it is connected to the rectifier bridges. The ZSBTs are employed between the rectifiers and the DC load. Considering the typical operation frequency of auto-transformer (360 Hz~800 Hz), the adoption of a high frequency transformer core may significantly reduce core size and iron loss. However, a trade-off of cost, flux density and operating frequency has to be made, and thus 0.2 mm silicon stripe has been chosen as autotransformer core since its operation frequency range is 50 Hz ~ 2 kHz [16]. Eq. (12) indicates that the fundamental frequency of ZSBT winding is the tripled frequency of power source, so the high frequency magnet material can cover the maximum frequency 2.4 kHz for ZSBT. Ferrite is employed in the experiments for ZSBT due to the cheap price and the high operation frequency. The size and weight of the autotransformer and ZSBT are listed in Table I and Table II. For a higher power application in the future, the core and winding will be designed much larger than those in the experiments (i.e. 18 kW).

Fig. 8 shows the experimental results of the proposed ATRU system at full load condition. It can be seen from Fig. 8 that the experimental results are in line with the simulation results shown in Fig. 6. The THD of the line current in Fig. 8 (a) at full load condition is 6.31%, which has met the requirement (THD $\leq$ 10 %). Meanwhile, the output voltage shown in Fig. 8(c) indicates that the ripple voltage is about 0.8% in respect to the DC value. The Fast Fourier Transform (FFT) analysis results of the input current are shown in Fig. 8(b), which demonstrates that the major harmonics are 23th and 25th as discussed as previously. However, the 5th and 7th order harmonics are still presents in the current spectrum due to the magnetic asymmetry of the autotransformer three-limb core. Otherwise, the preexisting unbalance source voltage and winding turn integration error may lead to unbalanced magnitudes of the input voltage. This will also contribute to low order harmonics in the current [17], [18].

When there is a step load current change from 2.5 kW to

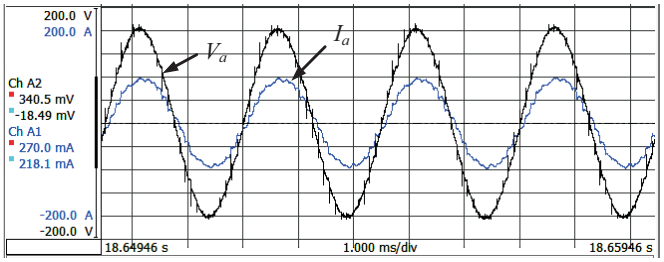

(a)

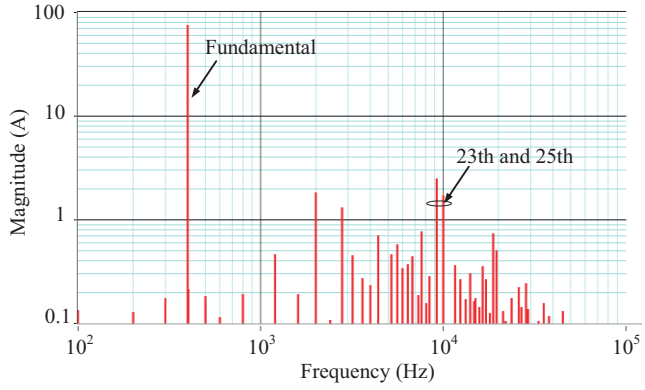

(b)

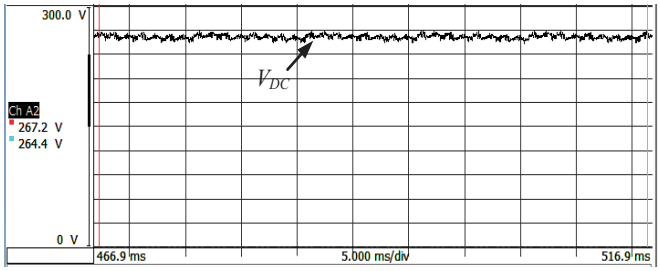

(c)

Fig. 8. Experimental results of the 24-pulse autotransformer rectifier unit at full load: (a) phase A input current [20 A/div], input voltage [20 V/div], and time [1 ms/div], (b) phase A current spectrum [20 A/div], and (c) auto-transformer rectifier unit output voltage [30 V/div], and time [5 ms/div].

full load under the normal working frequency (400 Hz) conditions, the current THD and the power factor are relatively independent of the output power, as shown in Fig. 9 and Fig. 10. The input current THD is decreased from 7.34% to 6.31% and the power factor is increased from 0.96 to 0.99, when the power increases to 18 kW. The measured efficiency that is depicted in Fig. 11 has a flat value, indicating that the circuit efficiency is dependent on the output power variation.

All these experimental results have verified the effectiveness of the proposed topology under different power levels. It is clear that the proposed 24-pulse autotransformer based rectifier shows good performance in terms of harmonic eliminations, and also to be cost-effective.

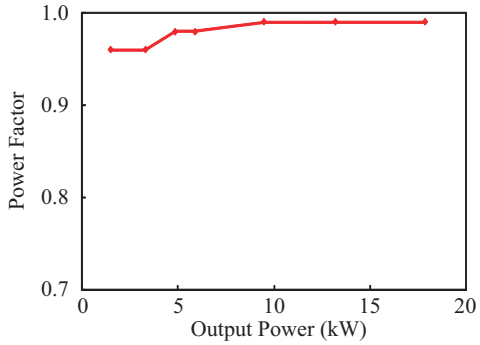

Fig. 9. Power factor of the 24-pulse autotransformer rectifier unit versus output power.

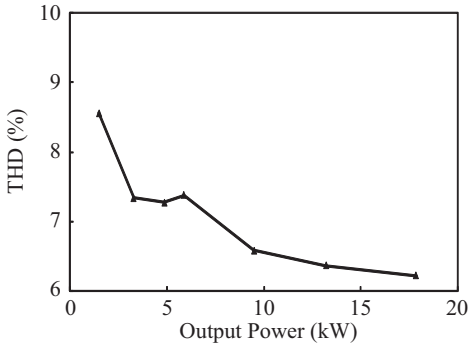

Fig. 10. Total harmonic distortion (THD) of the input current versus the output power.

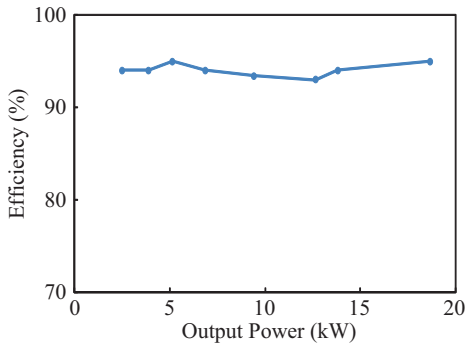

Fig. 11. Efficiency of the 24-pulse autotransformer rectifier Unit versus output power.

V. Conclusion

In this paper, an improved 24-pulse autotransformer based rectifier unit, which provides a cost-effective solution for aircraft applications, has been proposed. By using zero sequence blocking transformers connected directly with rectifier bridges, the magnetic components for paralleled rectifier bridges are reduced from six to four. This will contribute to a reduction of both the cost and the weight of the entire system. A thorough analysis of the proposed zero sequence blocking transformer has been presented in this

paper, which shows that the kVA rating of the zero sequence blocking transformer is only 0.034 times of the output power. Both simulation and experimental results have verified the effectiveness of the proposed zero sequence blocking transformer configuration. The system can also maintain a high overall efficiency and a high power factor for a wide operating range. It can also be concluded from the experimental results that the total harmonic distortion of the line current is 6.31%, which has met the design target (THD ≤ 10 %) at full load condition, and the harmonics lower than the 23^{th} order in the AC supply current have been eliminated effectively with the proposed topology.

REFERENCES

[1] A. Uan-Zo-li, R. Burgos, F. Wang, D. Boroyevich, F. Lacaux, and A. Tardy, "Comparison of prospective topologies for aircraft autotransformer-rectifier units," in *Proc. of IEEE IECON '03*, pp. 1122-1127, 2003.

[2] I. Weimer, ''Electrical power technology for the more electric aircraft," in *Proc. of IEEE DASC'93*, pp. 445-450, Oct. 1993.

[3] L. Faleiro, "Beyond the more electric aircraft," *Aerospace America*, Sept. 2005.

[4] C. Adams, "A380 'more electric' aircraft," *Avionics Mag.*, Oct. 2001.

[5] D. Paice. *Power Electronic Converter Harmonies Multipulse Method for Clean Power*. Wiley - IEEE, 1996.

[6] B. Singh, S. Gairola, B. N. Singh, A. Chandra, and K. Al-Haddad, "Multi-pulse AC-DC converters for improving power quality: A review," *IEEE Trans. Power Electron.,* vol. 23, no. 1, pp. 260-281, Jan. 2008.

[7] B. S. Lee, P. N. Enjeti, and I. J. Pitel, "A new 24-pulse diode rectifier system for AC motor drives provides clean power utility interface with low kVA components" in *Proc. of IEEE Thirty-first IAS Annual Meeting*, pp. 1024-1031,Oct. 1996.

[8] F. Meng, S. Yang, and W. Yang, "Modeling for a multitap interphase re-actor in a multipulse diode bridge rectifier," *IEEE Trans. Power Electron.* ,vol. 24, no. 9, pp. 2171–2177, Sep. 2009.

[9] I.G. Park and S. I. Kim, "Modeling and analysis of multi-interphase transformers for connecting power converters in parallel," in *Proc. of IEEE PESC '97*, vol. 2, pp. 1164-1170, Jun. 2010.

[10] B. Singh, G. Bhuvaneswari, and V. Garg, "Harmonic mitigation using 12-pulse AC-DC converter in vector-controlled induction motor drives," *IEEE Trans. Power Delivery,* vol. 21, no.3, pp. 1483-1492, Jul. 2006.

[11] O. N. Acosta, "Interphase transformer for multiple connected power rectifiers," *IEEE Trans. Industry and General Applications.,* vol. IGA-1, no. 6, pp. 423-428, Nov. 1965.

[12] C. M. Young, M. H. Chen, C. H. Lai, and D. C. Shih, "A novel control for active interphase transformer using in a 24-pulse converter," in *Proc. of IEEE IPEC*, pp. 2086-2091, Jun. 2010.

[13] X.H. Wu, P.P. Cai, and X.B. Zhang, "Design and analysis of an auto-transformer based 24-pulse rectifier," in *Proc. of IEEE ICECE*, pp. 3529-3532, Jun. 2010.

[14] B. Singh, G. Bhuvaneswari, V. Garg, and A. Chandra, "Star connected autotransformer based 30-pulse AC-DC converter for power quality improvement in vector controlled induction motor drives," in *Proc. of IEEE Power India*, 2006.

[15] G. Seguier, *Power Electronic Converters AC/DC Conversion*. New York McGraw-Hill, 1986.

[16] C.McLyman, *Transformer and Inductor Design Handbook*, 3rd ed. New York: Marcel Dekker, 2004.

[17] G.Gong, U.Drofenik, and J.W. Kolar, "12-Pulse rectifier for more electric aircraft applications" in *Proc. of IEEE Industrial Technology*, pp. 1096-1101, Dec. 2003.

[18] S.G. Jeong and J.Y. Choi, "Line current characteristics of three-phase uncontrolled rectifiers under line voltage unbalance condition" *IEEE Trans. Power Electron.,* vol. 17, no. 6, pp. 935-945, Nov. 2002.